NANO · MICRO

small

Supporting Information

Synthetic Tailoring of Ionic Conductivity in Multicationic Substituted, High-Entropy Lithium Argyrodite Solid Electrolytes

Jing Lin, Mareen Schaller, Gennady Cherkashinin, Sylvio Indris, Jianxuan Du, Clemens Ritter, Aleksandr Kondrakov, Jürgen Janek, Torsten Brezesinski* and Florian Strauss*

Supporting Information

Synthetic Tailoring of Ionic Conductivity in Multicationic Substituted, High-Entropy Lithium Argyrodite Solid Electrolytes

Jing Lin,[a] Mareen Schaller,[b] Gennady Cherkashinin,[c] Sylvio Indris,[b] Jianxuan Du,[a] Clemens Ritter,[d] Aleksandr Kondrakov,[a,e] Jürgen Janek,[a,f] Torsten Brezesinski,[a]* and Florian Strauss[a]*

[a] Battery and Electrochemistry Laboratory (BELLA), Institute of Nanotechnology (INT), Karlsruhe Institute of Technology (KIT), Hermann-von-Helmholtz-Platz 1, 76344 Eggenstein-Leopoldshafen, Germany.

[b] Institute for Applied Materials–Energy Storage Systems (IAM-ESS), Karlsruhe Institute of Technology (KIT), Hermann-von-Helmholtz-Platz 1, 76344 Eggenstein-Leopoldshafen, Germany.

[c] Advanced Thin Film Technology, Institute of Materials Science, Technical University of Darmstadt, Alarich-Weiss Str. 2, 64287 Darmstadt, Germany.

[d] Institut Laue-Langevin, 38042 Grenoble Cedex 9, France.

[e] BASF SE, Carl-Bosch-Str. 38, 67056 Ludwigshafen, Germany.

[f] Institute of Physical Chemistry & Center for Materials Research (ZfM/LaMa), Justus-Liebig-University Giessen, Heinrich-Buff-Ring 17, 35392 Giessen, Germany.

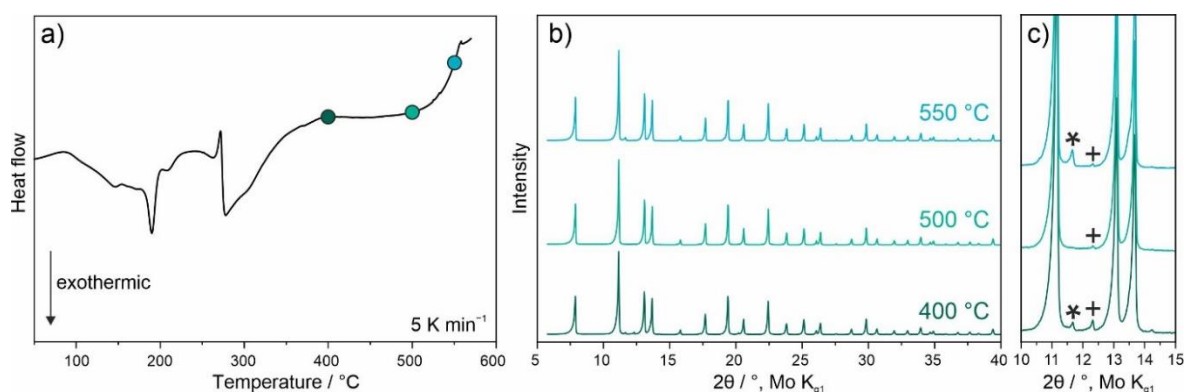*Corresponding authors: torsten.brezesinski@kit.edu, florian.strauss@kit.edu

Figure S1. a) DSC trace of the precursor mixture. b) XRD patterns after annealing at different temperatures as indicated in a). c) Magnified view to visualize the additional reflections arising from Li_2S (asterisk) and LiI (cross) impurities. Ionic conductivities of the same samples from cold-pressed pellets are given in **Table S1**.
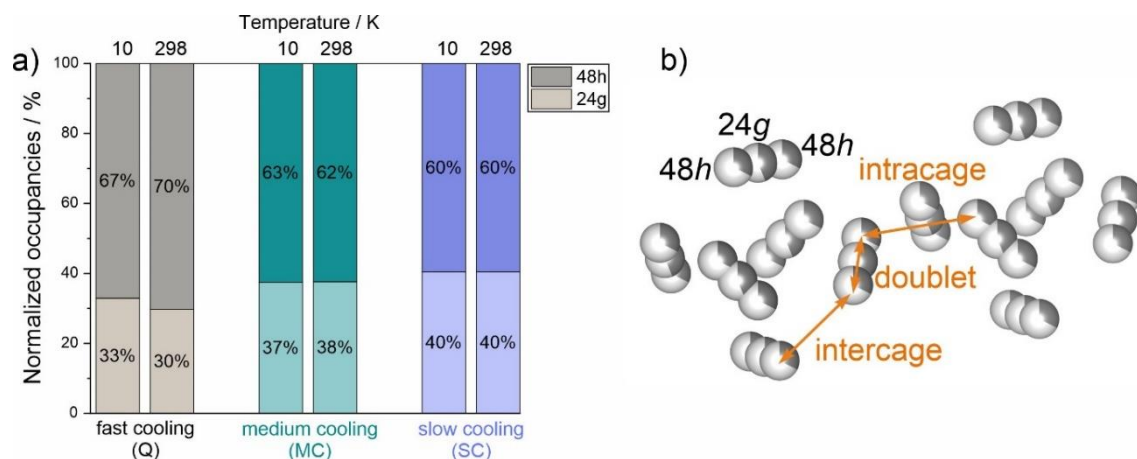
Figure S2. a) Normalized Li occupancies over the Wyckoff positions 48*h* and 24*g*. b) Two neighboring Li cages. The different transport (jump) pathways and sites are indicated.
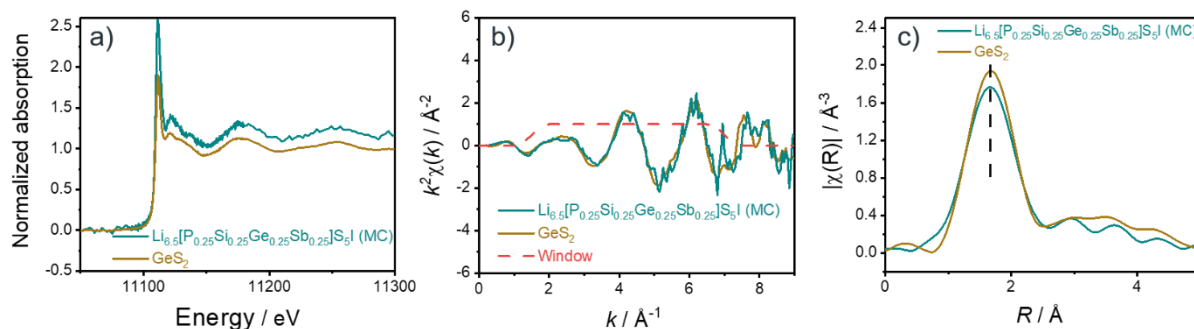

Figure S3. a) Ge K-edge XANES and b) k^2-weighted EXAFS [χ(k)] spectra. c) Corresponding magnitudes of the Fourier transform for $Li_{6.5}[P_{0.25}Si_{0.25}Ge_{0.25}Sb_{0.25}]S_5I$ (MC) (cyan) and the GeS_2 reference material (brown).
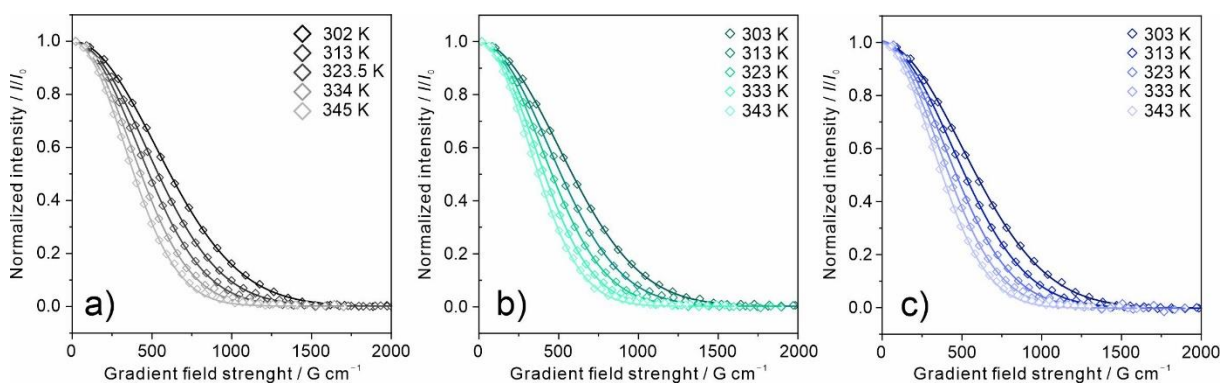

Figure S4. Results from temperature-dependent ^7Li PFG NMR spectroscopy measurements for a) fast- (Q), b) medium- (MC) and c) slow-cooled (SC) samples, with symbols and lines representing experimental and calculated data, respectively.
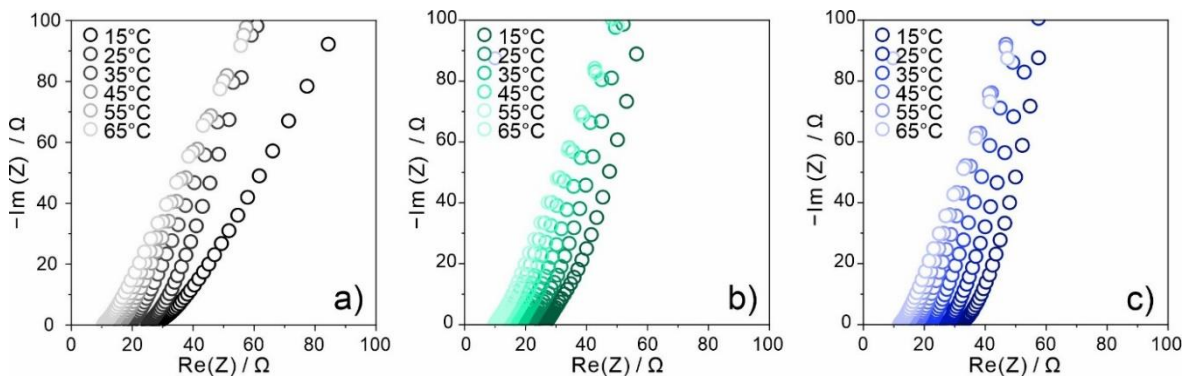
Figure S5. Nyquist plots of the electrochemical impedance measured between 15 and 65 °C for a) fast- (Q), b) medium- (MC) and c) slow-cooled (SC) samples.
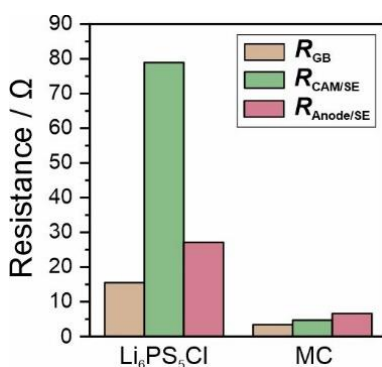

Figure S6. Calculated resistances from the impedance spectra in **Figure 8b** for the Li$_{6.5}$[P$_{0.25}$Si$_{0.25}$Ge$_{0.25}$Sb$_{0.25}$]S$_5$I- (MC) and Li$_6$PS$_5$Cl-based cells after the first cycle.
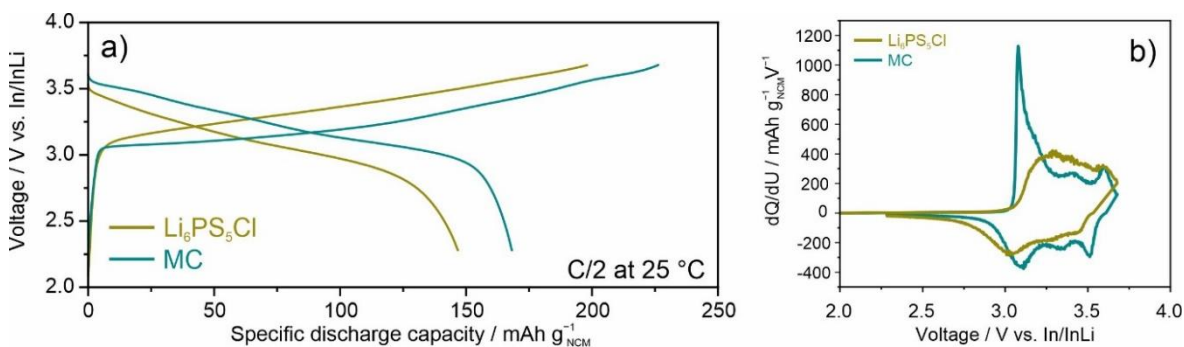

Figure S7. a) First- and second-cycle voltage profiles at 25 °C and C/2 rate and b) corresponding differential capacity plots for the Li$_{6.5}$[P$_{0.25}$Si$_{0.25}$Ge$_{0.25}$Sb$_{0.25}$]S$_5$I- (MC) and Li$_6$PS$_5$Cl-based cells.
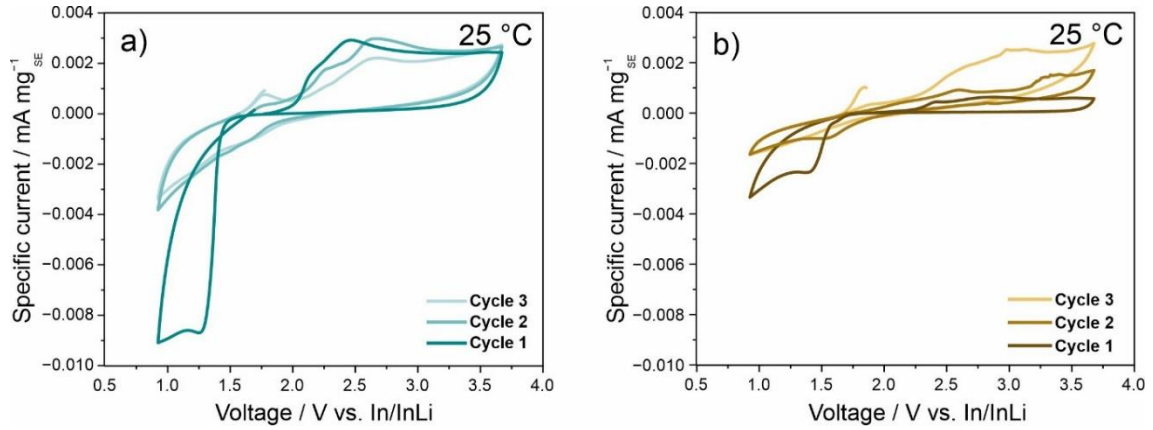
Figure S8. CV curves at 0.1 mV s^{-1} and 25 °C for a) Li$_{6.5}$[P$_{0.25}$Si$_{0.25}$Ge$_{0.25}$Sb$_{0.25}$]S$_5$I (MC) and b) Li$_6$PS$_5$Cl. Note that mixtures of SE and carbon black were used as working electrode.

Table S1. Ionic conductivities determined from cold-pressed pellets annealed at different temperatures (see **Figure S1**).

Annealing temperature / °C	σ_{ion} / mS cm^{-1}
400	7.6
500	10.7
550	8.7

Table S2. Lattice parameters for the samples prepared with different cooling rates, with MC data taken from the literature.[1]

Sample	a / Å (T = 298 K)	a / Å (T = 10 K)
Quenched (Q)	10.29903(7)	10.25347(4)
Medium cooled (MC)	10.29714(9)	10.24932(5)
Slow cooled (SC)	10.30141(7)	10.25696(6)

Table S3. Structural parameters for Li$_{6.5}$[Si$_{0.25}$Ge$_{0.25}$P$_{0.25}$Sb$_{0.25}$]S$_5$I (Q) from Rietveld analysis of NPD data collected at T = 298 K.^{a}

Atom	Wyckoff site	x	y	z	B_{iso} / Å^2	Occ
I1	4d	0.25	0.25	0.75	1.64(4)	0.11(2)
I2	4a	0	0	0	2.19(3)	0.88(7)
S1	4d	0.25	0.25	0.75	1.64(4)	0.88(7)
S2	4a	0	0	0	2.19(3)	0.11(2)
S3	16e	0.1237(6)	−0.1237(6)	0.6237(6)	1.26(4)	1
Si1	4b	0	0	0.5	0.96(0)	0.25
Ge1	4b	0	0	0.5	0.96(0)	0.25
P1	4b	0	0	0.5	0.96(0)	0.25

Sb1	4*b*	0	0	0.5	0.96(0)	0.25
Li1	48*h*	0.2948(9)	0.0202(8)	0.7051(3)	3.67(4)	0.38(0)
Li2	24*g*	0.25	0.0205(4)	0.75	1.57(7)	0.32(0)

[a] *F*−43*m* space group, a = 10.29903(7) Å, V = 1092.421(17) Å^3, ρ = 2.406 g cm^{-3}, R_{wp} = 7.58%, χ^2 = 4.060.

Table S4. Structural parameters for Li$_{6.5}$[Si$_{0.25}$Ge$_{0.25}$P$_{0.25}$Sb$_{0.25}$]S$_5$I (Q) from Rietveld analysis of NPD data collected at T = 10 K.[a]

Atom	Wyckoff site	x	y	z	B_{iso} / Å^2	Occ
I1	4*d*	0.25	0.25	0.75	0.93(9)	0.14(1)
I2	4*a*	0	0	0	1.04(6)	0.85(9)
S1	4*d*	0.25	0.25	0.75	0.93(9)	0.85(9)
S2	4*a*	0	0	0	1.04(6)	0.14(1)
S3	16*e*	0.1261(2)	−0.1261(2)	0.6261(2)	0.57(6)	1
Si1	4*b*	0	0	0.5	0.10(4)	0.25
Ge1	4*b*	0	0	0.5	0.10(4)	0.25
P1	4*b*	0	0	0.5	0.10(4)	0.25
Sb1	4*b*	0	0	0.5	0.10(4)	0.25
Li1	48*h*	0.2958(2)	0.0210(2)	0.7041(8)	1.93(2)	0.36(0)
Li2	24*g*	0.25	0.0242(0)	0.75	0.71(6)	0.36(0)

[a] *F*−43*m* space group, a = 10.25347(4) Å, V = 1078.984(10) Å^3, ρ = 2.439 g cm^{-3}, R_{wp} = 3.23%, χ^2 = 3.329.

Table S5. Structural parameters for Li$_{6.5}$[Si$_{0.25}$Ge$_{0.25}$P$_{0.25}$Sb$_{0.25}$]S$_5$I (SC) from Rietveld analysis of NPD data collected at T = 298 K.[a]

Atom	Wyckoff site	x	y	z	B_{iso} / Å^2	Occ
I1	4*d*	0.25	0.25	0.75	1.56(9)	0.12(7)
I2	4*a*	0	0	0	2.09(6)	0.87(2)
S1	4*d*	0.25	0.25	0.75	1.56(9)	0.87(2)
S2	4*a*	0	0	0	2.09(6)	0.12(7)
S3	16*e*	0.1234(9)	−0.1234(9)	0.6234(9)	1.16(1)	1
Si1	4*b*	0	0	0.5	0.87(8)	0.25
Ge1	4*b*	0	0	0.5	0.87(8)	0.25
P1	4*b*	0	0	0.5	0.87(8)	0.25
Sb1	4*b*	0	0	0.5	0.87(8)	0.25

Li1	48h	0.2967(5)	0.0200(2)	0.7032(5)	3.09(5)	0.32(2)
Li2	24g	0.25	0.0184(9)	0.75	1.57(9)	0.43(8)

[a] $F–43m$ space group, a = 10.30141(7) Å, V = 1093.178(17) Å^3, ρ = 2.407 g cm^{-3}, R_{wp} = 3.92%, χ^2 = 2.807.

Table S6. Structural parameters for Li$_{6.5}$[Si$_{0.25}$Ge$_{0.25}$P$_{0.25}$Sb$_{0.25}$]S$_5$I (SC) from Rietveld analysis of NPD data collected at T = 10 K.[a]

Atom	Wyckoff site	x	y	z	B_{iso} / Å^2	Occ
I1	4d	0.25	0.25	0.75	0.92(9)	0.13(5)
I2	4a	0	0	0	1.07(7)	0.86(5)
S1	4d	0.25	0.25	0.75	0.92(9)	0.86(5)
S2	4a	0	0	0	1.07(7)	0.13(5)
S3	16e	0.1254(3)	−0.1254(3)	0.6254(3)	0.49(8)	1
Si1	4b	0	0	0.5	0.15(8)	0.25
Ge1	4b	0	0	0.5	0.15(8)	0.25
P1	4b	0	0	0.5	0.15(8)	0.25
Sb1	4b	0	0	0.5	0.15(8)	0.25
Li1	48h	0.2973(9)	0.0199(5)	0.7026(1)	1.85(8)	0.32(2)
Li2	24g	0.25	0.0211(3)	0.75	1.54(4)	0.43(8)

[a] $F–43m$ space group, a = 10.25696(6) Å, V = 1079.088(15) Å^3, ρ = 2.436 g cm^{-3}, R_{wp} = 3.08%, χ^2 = 3.122.

Table S7. Li-Li jump distances at T = 298 and 10 K for the Li$_{6.5}$[Si$_{0.25}$Ge$_{0.25}$P$_{0.25}$Sb$_{0.25}$]S$_5$I samples prepared with different cooling rates, with MC data taken from the literature.[1] For comparison, the corresponding jump distances in Li$_6$PS$_5$I are also given (T = 300 K, from ref. [2]).

T / K	48h-48h / Å	Intracage / Å	Intercage / Å
298 (Q)	1.31(4)	2.69(3)	3.28(3)
298 (MC)	1.39(6)	2.64(2)	3.24(2)
298 (SC)	1.361(2)	2.67(3)	3.25(3)
10 (Q)	1.33(3)	2.66(3)	3.27(3)
10 (MC)	1.39(2)	2.63(2)	3.23(1)
10 (SC)	1.38(1)	2.65(2)	3.22(2)
300 (Li$_6$PS$_5$I)	1.25	2.57	3.35

Table S8. Binding energies from fitting of XPS data. Major and minor indicate that two contributions were assumed in the curve fitting.

Element	BE / eV (Q)	BE / eV (MC)	BE / eV (SC)
O 1s	531.8 (major) 532.8 (minor)	532.0 (major) 533.0 (minor)	532.0 (major) 533.1 (minor)
Sb 3d	530.2 (major) 529.3 (minor)	530.4 (major) 529.5 (minor)	530.3 (major) 529.5 (minor)
S 2p	161.3 (major) 163.3 (minor)	161.5 (major) 163.7 (minor)	161.4 (major) 163.7 (minor)
P 2p	132.1	132.4	132.2
Si 2p	100.9 (major) 102.5 (minor)	101.0 (major) 102.7 (minor)	101.0 (major) 102.7 (minor)
I 4d	48.6 (major) 49.1 (minor)	49.4 (major) 49.9 (minor)	49.3 (major) 49.9 (minor)
Sb 4d	34.1 (major) 33.2 (minor)	34.3 (major) 33.3 (minor)	34.2 (major) 33.3 (minor)
Ge 3d	30.7	30.9	30.8

Table S9. Surface composition of the samples prepared with different cooling rates in units of at.% from XPS.

Sample	Li	P	Si	Ge	Sb	S	I	O
Q	39.1	1.3	1.9	1.7	2.9	32.4	12.3	8.3
MC	37.9	1.6	3.1	1.8	2.9	32.1	12.0	8.7
SC	35.5	1.4	2.0	1.6	2.0	36.6	9.4	11.6

[1]   J. Lin, G. Cherkashinin, M. Schäfer, G. Melinte, S. Indris, A. Kondrakov, J. Janek, T. Brezesinski, F. Strauss, ACS Materials Lett. **2022**, *4*, 2187.

[2]   N. Minafra, M. A. Kraft, T. Bernges, C. Li, R. Schlem, B. J. Morgan, W. G. Zeier, Inorg. Chem. **2020**, *59*, 11009.